

NEW SILICON CELL DESIGN CONCEPTS FOR >20 PERCENT AMI EFFICIENCY

M. Wolf
University of Pennsylvania
Philadelphia, Pennsylvania

SUMMARY

The basic design principles for obtaining high efficiency in silicon solar cells are reviewed. They critically involve very long minority carrier lifetimes, not so much to attain high collection efficiency, but primarily for increased output voltages. Minority carrier lifetime, however, is sensitive to radiation damage, and particularly in low resistivity silicon, on which the high efficiency design is based. Radiation resistant space cells will therefore have to follow differing design principles than high efficiency terrestrial cells.

DESIGN VIEWPOINTS DERIVABLE FROM AN IDEALIZED CELL STRUCTURE

In the simple solar cell structure, which consists only of one layer for each of the three regions (front, depletion, and base region)¹⁾, three light generated current components flow (one each from the three regions), which all need to be maximized for best collection efficiency. In addition, two injection current components flow in forward bias operation (one into the base and one into the front region) which need to be minimized to achieve high output voltages. Optimum performance for terrestrial applications or BOL space service is achieved when the surface recombination velocities both at the front and at the back surfaces are zero (Fig. 1). Then the device design involves a trade-off between light generated and open circuit voltage, to attain maximum power output. This trade-off involves primarily the thickness of the base region. The optimum design also indicates impurity concentrations just at the onset of Auger recombination, equal in both the front and the base regions, when secondary, technology dependent effects, such as series resistance related losses, are dealt with separately.

The consideration of the simple device structure shows that the basic device does not require the properties of an "emitter" for the front region, and that the open circuit voltage monotonously increases with increasing minority carrier lifetime, while the collection efficiency essentially saturates as long recognized²⁾. To gain the highest possible performance, the highest technologically achievable minority carrier lifetime is thus needed.

While, principally, improved open circuit voltages are expected from increasing dopant concentrations, the onset of direct, band-to-band Auger recombination sets a basic limit to this trend,²⁾ (Fig. 2), as does bandgap narrowing³⁾. Thus, an optimum impurity concentration will be reached just before Auger recombination causes a downturn of the power output with a further increase of the impurity concentration. In consequence of this observation, a high efficiency solar cell design should avoid very high doping concentrations at which the heavy doping effects have a significant influence on the device performance. There exist some doubts, however, on the currently accepted values of Auger recombination⁴⁾ and bandgap narrowing⁵⁾ in depen-

dence on the dopant concentration. After better information on these heavy doping effects has been attained, the solar cell design philosophies might change slightly.

Both the maximum idealized efficiency and the dopant concentration at which this efficiency is obtained, (Fig. 3), depend on the minority carrier lifetime model chosen. The three models for the dependency of the minority carrier lifetime on dopant concentration, on which the three efficiency curves of Fig. 3 are based, are shown in Fig. 4⁶⁾. (Fig. 3 is based on a more detailed solar cell model outlined in the next section, but similar curves could have been obtained with the simple model).

REALISTIC STRUCTURES FOR HIGH EFFICIENCY TERRESTRIAL SOLAR CELLS

After the considerations on the idealized structure, the question arises to what degree such high performance may be approximated in realistic cell structures?

The first obstacle to zero surface recombination velocity on the back surface, appears to be the ohmic contact which represents a surface recombination velocity near 10^6 cm s^{-1} . A suitable high/low junction structure with a third, more heavily doped base layer of significant thickness, can accomplish a transport velocity transformation from values near 10^6 cm s^{-1} down to 20 cm s^{-1} at the interface between the narrow base layer and the high/low junction (Fig. 5). This is an adequately low value for close approximation of zero surface recombination velocity at the back of the base layer.⁶⁾

For the front, however, a similar approach is not appropriate, as the relatively thick third, more heavily doped layer would diminish the collection efficiency. However, a structure as illustrated in Fig. 6 could form an appropriate remedy. Here, the third layer exists only under the ohmic contacts which are represented by the grid line and bus line pattern on the front surface of the cell. The light-exposed surface is located directly on the less heavily doped front layer. Its surface recombination velocity, as it results from the fabrication processes applied, would normally be too high to allow adequately high performance. Particularly the influence on the saturation current which determines the open circuit voltage, would reduce performance. Thus, adequate means for reduction of the surface recombination velocity to values near 100 cm s^{-1} on the open front surface will still be needed. Doped oxides or induced accumulation layers (MIS structures) may accomplish this result. MIS approaches can also be used to reduce the effect of the high surface recombination velocity of the ohmic contact, similar to the high/low junction-third layer combination.

Appropriately applying these measures in combination can achieve a performance comparable to that of the idealized device of Fig. 1. It may be noted that, in the computation of the idealized efficiency data, a textured front surface (oblique photon penetration) and an internally optically reflecting back surface were included. Also, for a realistically achievable cell, including front surface shading by metallization, series resistance losses, a non-ideal antireflection coating, etc., the performance data have to be reduced to about 90% of the values given here.

CELL DESIGN FOR HIGH PERFORMANCE AFTER ENERGETIC PARTICLE EFFECTS

The high solar cell performance discussed in the preceding paragraphs, is achievable only with very large diffusion lengths in both the front and the base regions of the device. In most space missions, however, the radiation environment rapidly reduces the minority carrier lifetime (Fig. 7) ⁷). The original curves (solid lines of Fig. 7) apply to solar cells of rather limited diffusion lengths, while the devices discussed in the preceding paragraphs would start with substantially longer values. However, they would follow the dashed curve under the influence of nuclear particle flux until their approximation to the original straight line. Thus, for 1 MeV electron equivalent nuclear radiation fluxes, at the fluence level of 10^{15} to 10^{16} cm^{-2} , no advantage would be derived from the original high diffusion lengths. In design computations for a solar cell structure corresponding to Fig. 6 ⁶), a parametric study for the optimum base layer thickness as function of the minority carrier lifetime in the base was carried out (Fig. 8), yielding both the optimum base thickness and the maximum efficiency achievable for a given minority carrier lifetime. At a 1 MeV equivalent fluence of 10^{16} cm^{-2} , the minority carrier lifetime would have decreased to 35 ns according to Fig. 7, and the corresponding efficiency would be 14% with a base layer thickness of 30 μm .

It is evident that the design for optimum EOL (end of life) performance of silicon solar cells will require very thin silicon wafers, but will still not be able to exceed a performance level near 14% (AMO). It should be noted that the prior computations were carried out for optimum cell performance under AM1 conditions. It will be necessary to carry out similar computations for an optimum performance at EOL under AMO. In fact, the 26.7% (AM1) efficient cell shows 23.9% efficiency for AMO (BOL).

While the terrestrial solar cell optimization was based on the use of low resistivity silicon, it is well known that this type of silicon is more radiation sensitive than higher resistivity material (Fig. 9). Thus, a radiation resistant design may include a trade-off towards the use of higher resistivity material. While the damage coefficient for diffusion length (Fig. 9) is reduced by approximately a factor of 3 in going from 1Ω cm ($p = 1.5 \times 10^{16}$ cm^{-3}) to 10Ω cm resistivity ($p = 1.3 \times 10^{15}$ cm^{-3}), the minority carrier mobility decreases from approximately 1000 to 750 $\text{cm}^2 \text{V}^{-1}\text{s}^{-1}$, so that the effective change in the damage coefficient for minority carrier lifetime is only approximately 2.25. Nevertheless, this difference in minority carrier lifetime damage coefficient will have a significant influence on the ultimate design of a radiation hardened, high performance silicon solar cell.

CONCLUSION

The principles of radiation resistant silicon solar cell design are opposing those of high efficiency design, particularly in the areas of selected resistivities and minority carrier lifetimes. An optimum EOL cell design needs still to be derived, but it is likely to be based on very thin silicon wafers. A disadvantage will be that the optimum EOL designs for different radiation environments will differ, and will be far from optimum at BOL. On the other hand, an optimum EOL design may not show much output degradation throughout its life.

REFERENCES

1. M. Wolf, "Updating the limit efficiency of silicon solar cells", IEEE Trans. Electron Devices, vol. ED-27, pp. 751-759, Apr. 1980.
2. H. Fischer and W. Pschunder, "Impact of material and junction properties on silicon solar cell efficiencies", in Rec. 11th IEEE Photovoltaic Spec. Conf., pp. 25-31, 1975.
3. Lindholm, F.A., Li, S.S., and Sah, C.T., "Fundamental limitations imposed by high doping on the performance of pn junction silicon solar cells", *ibid.*, pp. 3-12.
4. J. Dziewior and W. Schmid, "Auger coefficients for highly doped and highly excited silicon", Appl. Phys. Lett., vol. 31, pp. 346-348, 1977.
5. Lanyon, H.P.D., "Bandgap reduction mechanism in heavily doped semiconductors", Rec. 15th IEEE Photovoltaic Spec. Conf., IEEE Cat. No. 81CH1644-4, pp. 415-421, May, 1981.
6. Bowler, D.L., and Wolf, M., "Interactions of efficiency and material requirements for terrestrial silicon solar cells", IEEE Trans. Components, Hybrids and Manuf'g. Technol., CHMT3, pp. 464-472, Dec. 1980.
7. Tada, H.Y., and Carter, J.R., Jr., "Solar Cell Radiation Handbook", Jet Propulsion Laboratory Publ'n., 77-56, Nov. 1977.

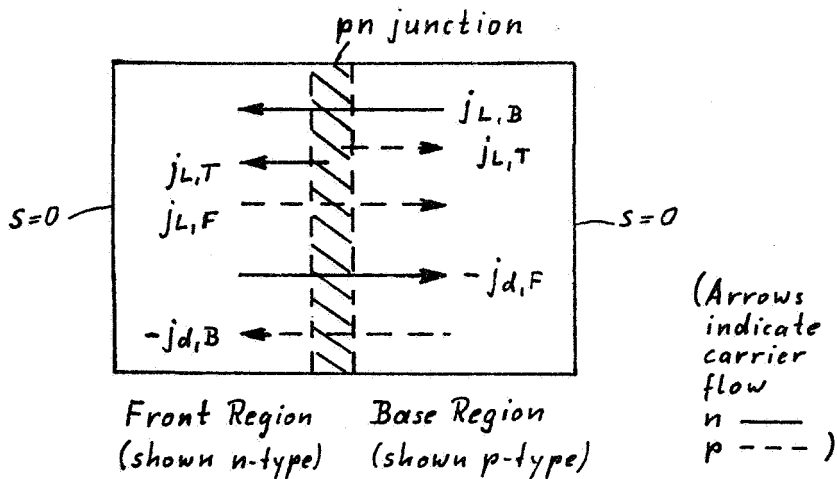


Fig. 1. Simplified ideal solar cell structure with zero surface recombination velocity at the outside boundary surfaces of both front region and base region.

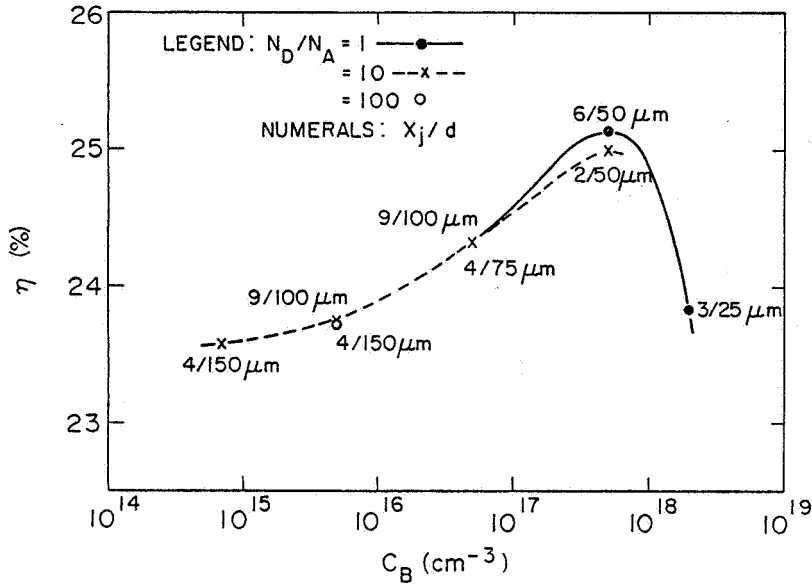


Fig. 2. Efficiency η of the idealized solar cell structure in dependence on the majority carrier concentration C_B in the base region. The numerals indicate the nominal front region thickness x_j and the total cell thickness d , at which optimum performance is achieved. Used as a parameter is the ratio of the impurity concentrations in the front (N_D) and base (N_A) regions, respectively.

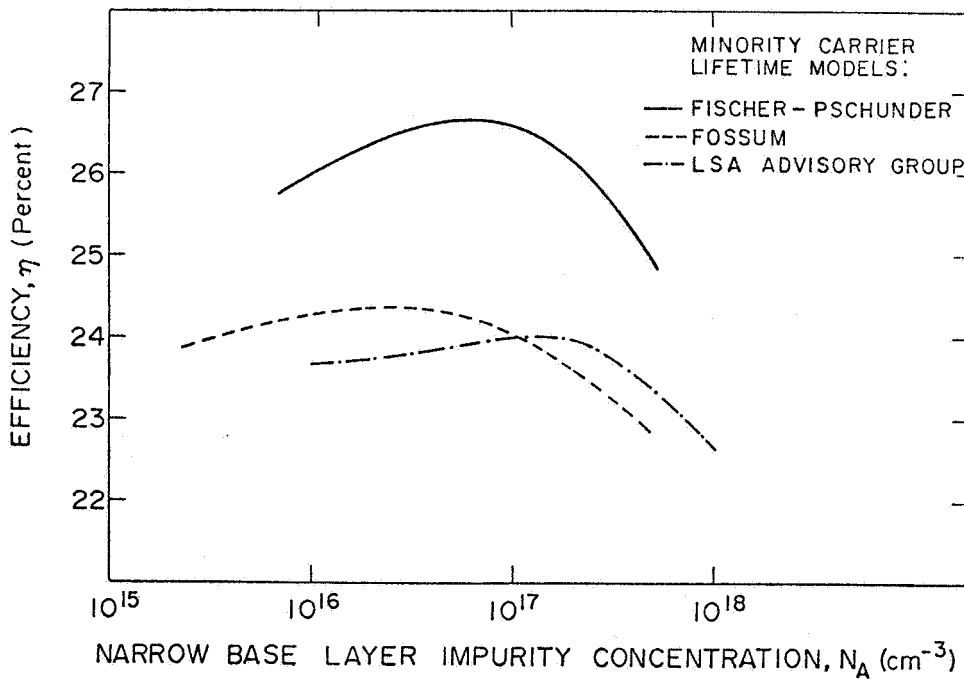


Fig. 3. Dependence of the efficiency versus base layer impurity concentration relationship on the minority carrier lifetime model used.

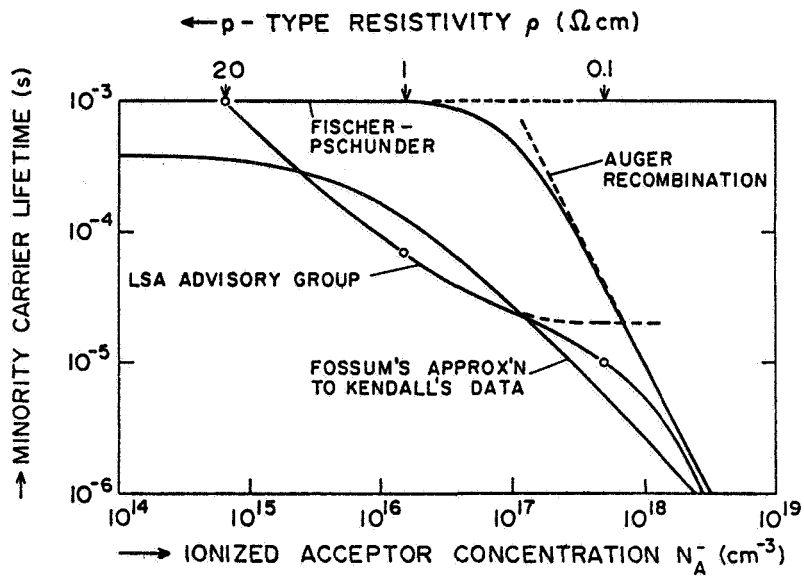


Fig. 4. The three minority carrier lifetime models used for Fig. 3. For details, see ref. 6.

		FRONT	PN	BASE 1	BASE 2	BASE 3	
u_d (←) [cm s ⁻¹]		200 (p)	52.6 (p)	225 (n)	52.8 (n)	2.1 · 10 ³ (n)	1 · 10 ⁶ (n)
$N_{D \text{ or } A}$ [cm ⁻³]		5 · 10 ¹⁷ - 2 · 10 ¹⁸		5 · 10 ¹⁶	—	2 · 10 ¹⁸	
$L_{p \text{ or } n}$ [μm]		36.3		226	88.4	34.5	
E [V cm ⁻¹]		1.93 · 10 ³		0	9.55 · 10 ³	0	
u_L (→) [cm s ⁻¹]		—	1 · 10 ⁹ (p)	1 · 10 ⁹ (n)	2.6 · 10 ³ (n)	1.03 · 10 ⁵ (n)	—
X [μm]		0	0.186	0.340	60	60.1	100
		$j_L = 39.79$ [mA cm ⁻²] (C.F.) = 0.847 $V_{oc} = 0.705$ [V] $\eta = 23.92$ [%]			FRONT: $j_L = 6.2$ [mA cm ⁻²]; $j_0 = 1.3 \cdot 10^{-15}$ [A cm ⁻²] BASE: $j_L = 31.0$ [mA cm ⁻²]; $j_0 = 5.7 \cdot 10^{-14}$ [A cm ⁻²]		

Fig. 5. Near optimum silicon solar cell structure (AM1) based on the lifetime model labeled LSA Advisory Group in Fig. 4.

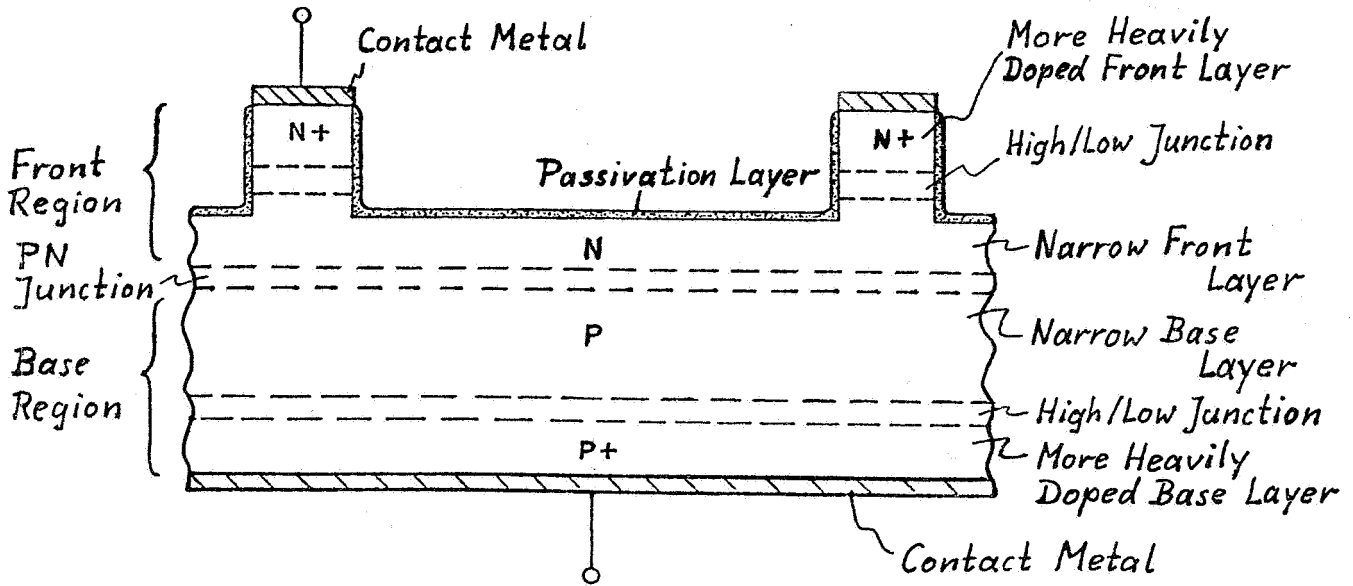


Fig. 6. Silicon solar cell structure for high efficiency.

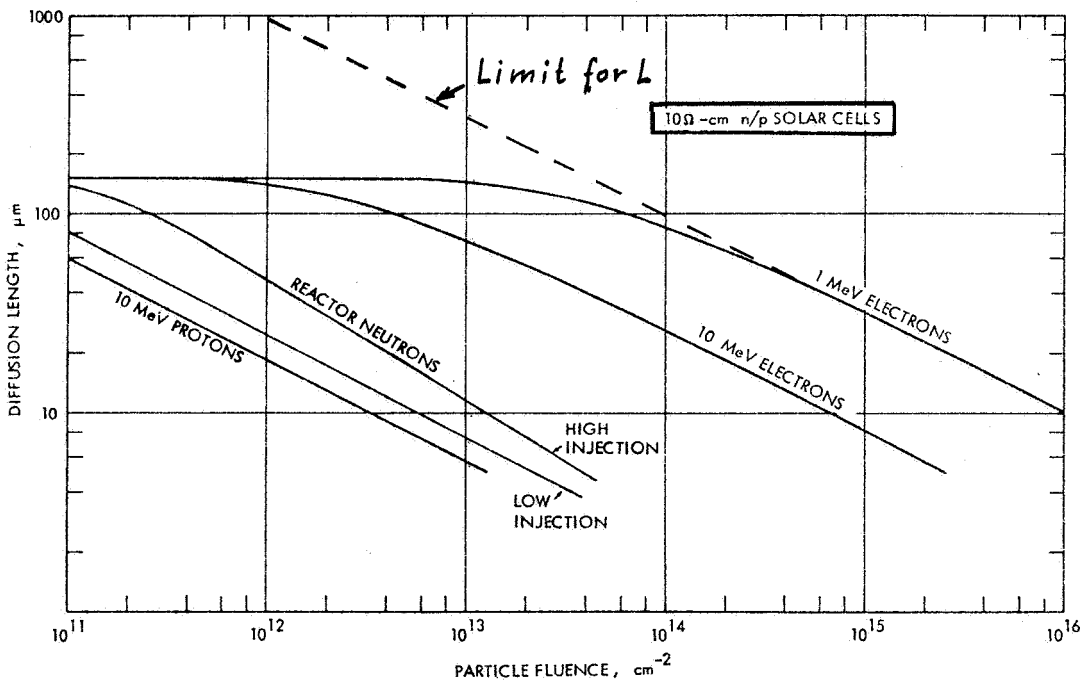


Fig. 7. Base region diffusion length L in 10Ω cm n/p Si solar cells as function of fluence for various energetic particles. From ref. 7.

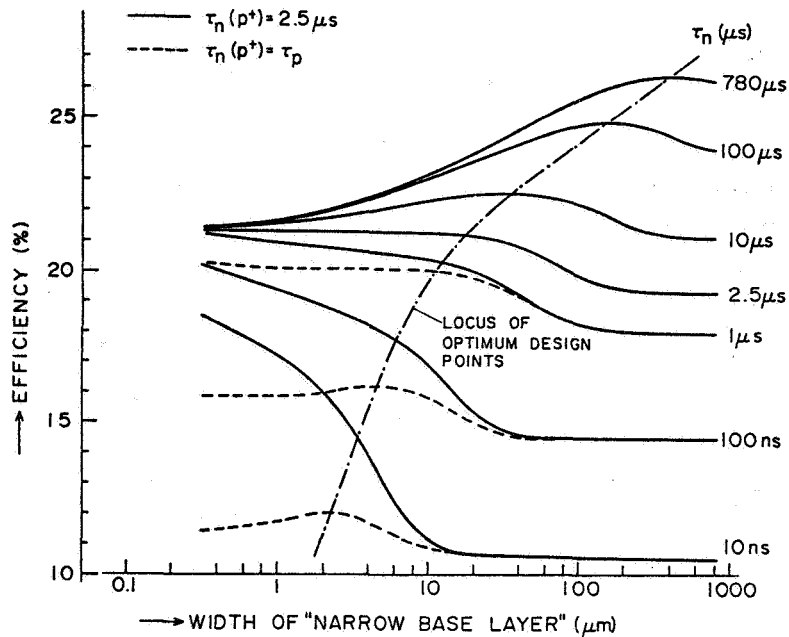


Fig. 8. Efficiency as function of the thickness of the less heavily doped base layer, with minority carrier lifetime in this layer as parameter. The dashed curves do not permit the lifetime in the more heavily doped base layer (p^+ layer) to exceed that of the p -layer. All other parameters kept constant.

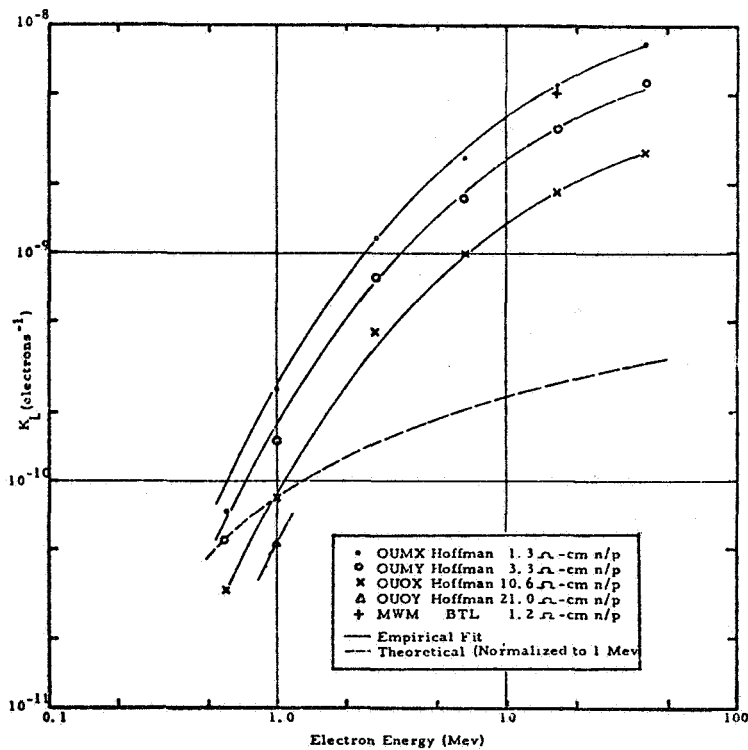


Fig. 9. Dependence of the damage coefficient K_L for diffusion length on electron energy and base region resistivity.

SURFACE EFFECTS IN HIGH-VOLTAGE SILICON SOLAR CELLS*

A. Meulenber, Jr., and R.A. Arndt
COMSAT Laboratories
Clarksburg, Maryland

EXTENDED ABSTRACT**

The influence of surface recombination velocity (SRV) on emitter dark current, and therefore on cell open-circuit voltage V_{OC} , has necessitated the use of low area "dot" contacts to reduce a major source of this dark current (ref. 1). Once the contact area is reduced sufficiently (or MIS contacts used to reduce SRV at the contacts), the major source of dark current from the emitter of a shallow junction solar cell is the oxide-silicon interface itself. (Heavy doping effects influence all cells, and Auger recombination is the major problem in deep junction solar cells.) Recombination and generation of carriers at this interface will influence both the blue response and the V_{OC} of such a cell, and therefore must be reduced as much as possible.

The SRV of a solar cell is increased and the blue response decreased by defect sites near the interface and by electric fields which draw minority carriers to the interface. The SRV contribution to the emitter dark current is also increased by heavy doping effects which create bandgap narrowing, even in the vicinity of the interface.

A series of experiments was performed in an attempt to reduce the surface recombination velocity of heavily doped silicon surfaces. Most of the effort involved diffused n^+p structures, but a comparison was also made with low doped MIS structures.

Antireflecting coatings deposited directly on a silicon surface provide poor interface characteristics so that passivating oxide generally needs to be grown prior to application of the AR coating. Solar cell processing at COMSAT Laboratories has traditionally used thermal oxidation of tantalum metal to form the AR coating and to passivate the surface simultaneously (ref. 2). During the early studies on this material, it was discovered by C-V techniques that significant negative charge was created and trapped in the Ta_2O_5 during the oxidation process (ref. 3). Cells fabricated in the early portion of this effort utilized this process without alteration.

To improve the traditional AR coating, it was found that application of positive static charge (ref. 4) to the front of the AR coating did not alter the cell characteristics. However, when the AR coating was subjected to a 750°C , 30-minute oxidation prior to forming the contact, the cell became quite sensitive to such surface charge. Figure 1 indicates the influence of positive charge on shallow junction solar cell I-V characteristics. Cells with junctions as deep as $1/5\ \mu\text{m}$ have displayed similar effects. As expected, the more

*This paper is based upon work performed at COMSAT Laboratories under the sponsorship of the Communications Satellite Corporation and supported in part by NASA Lewis under Contract NAS3-22217.

**Full text to appear in the 16th Photovoltaic Specialists Conference, San Diego, CA, September, 1982.

heavily doped surfaces showed the least response to charge. The oxidation step must either reduce or compensate the charge in the Ta_2O_5 or it must remove defect sites that pin the Fermi level locally at the interface. This oxidation step adds about 5 mV to the average open-circuit voltage even with no surface charge.

MIS cells have been fabricated (fig. 2) that exhibited dark currents lower than those in 650-mV, diffused cells.¹ The implication is that the SRV of the MIS structure is lower than that of diffused cells and/or that the inversion layer is better than the diffused layer. A third possibility is that simple oxidation of a heavily doped and/or diffused layer cannot provide a well-passivated surface.

Major conclusions of this study are as follows:

- a. Surface recombination velocity is the major limitation of shallow junction solar cells.
- b. Proper surface passivation allows significant influence on blue response and V_{OC} by use of static charge applied to the surface.
- c. Surface passivation of heavily diffused surfaces does not appear to break an apparent V_{OC} barrier for diffused cells at ~655 mV.
- d. MIS structures have shown greater potential for high V_{OC} , probably as a result of lower SRV at the oxide-silicon interface.

REFERENCES

1. Rittner, E. S.; Meulenbergh, A.; and Allison, J. F.: Dependence of Efficiency of Shallow Junction Silicon Solar Cells on Substrate Doping. *Journal of Energy*, vol. 5, no. 1, January-February 1981, pp. 9-14.
2. Revesz, A. G.; and Allison, J. H.: Electronic Properties of the Silicon-Thermally Grown Tantalum Oxide Interface. *IEEE Transactions on Electron Devices*, vol. ED-23, no. 5, May 1976, pp. 527-529.
3. Revesz, A. G.; Allison, J. F.; and Reynolds, J. H.: Tantalum Oxide and Niobium Oxide Antireflection Films in Silicon Solar Cells. *COMSAT Technical Review*, vol. 6, no. 1, Spring 1976, pp. 57-69.
4. Lam, Y. W.; Green, M. A.; and Davies, L. W.: Electrostatic Effects in Inversion-Layer Metal-Insulator-Semiconductor Solar Cells. *Applied Physics Letters*, vol. 37 (12), December 15, 1980, pp. 1087-1089.

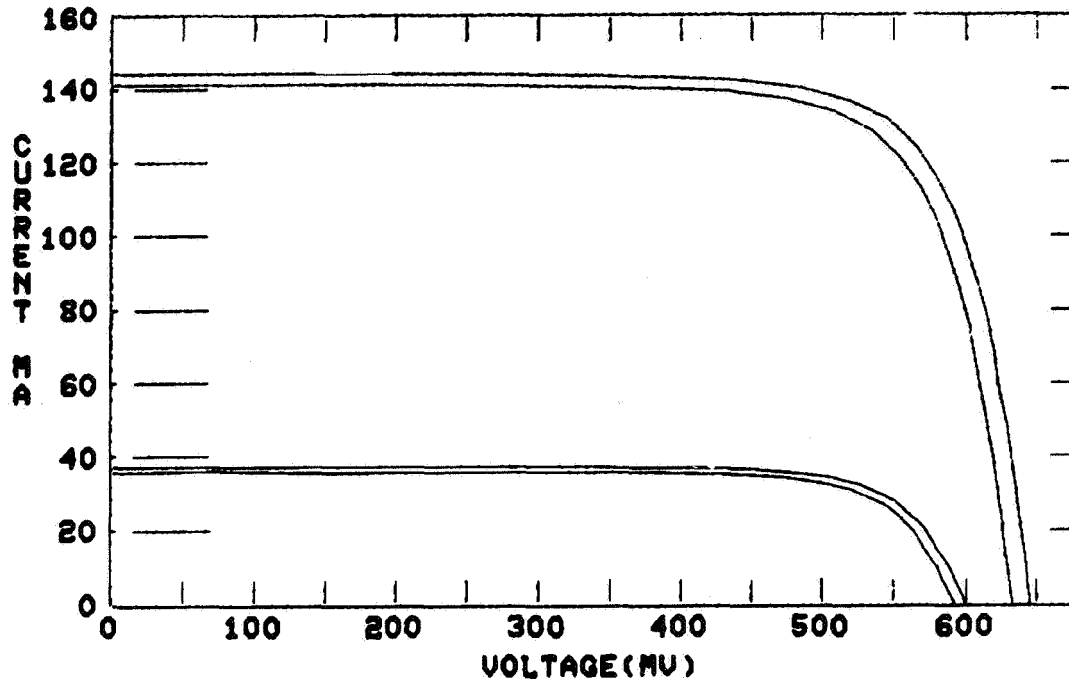


Figure 1. - The influence of positive surface charge on a shallow junction solar cell. The upper curve of each pair is for the cell when charged.

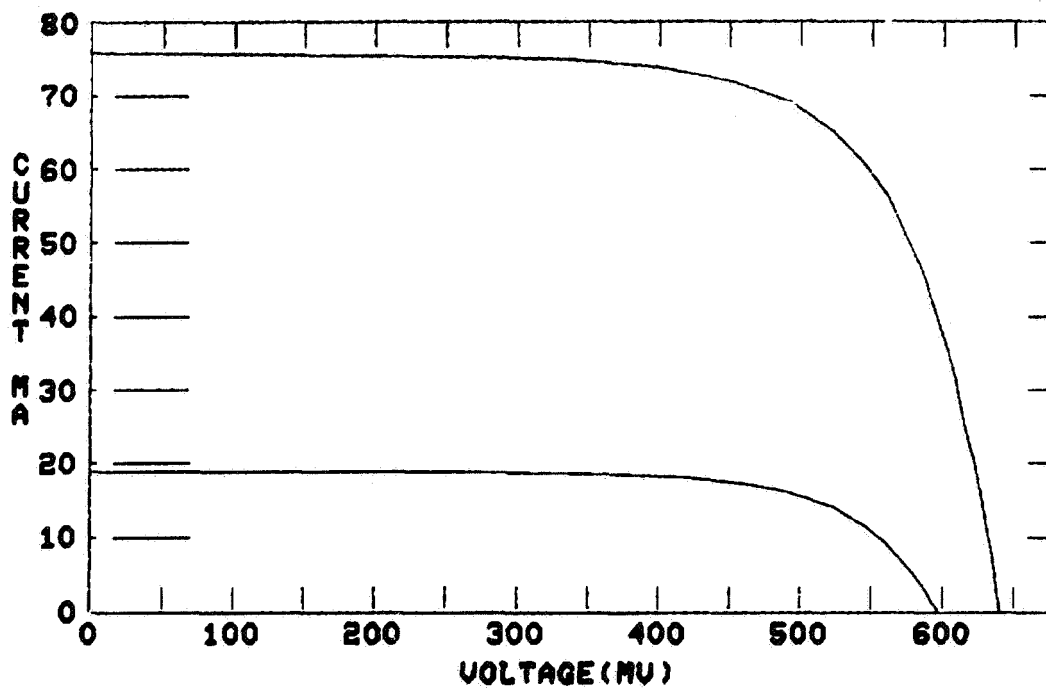


Figure 2. - The IV characteristics of an MIS cell (0.1 Ω -cm substrate, ~ 100 Å Er + ~ 50 Å Cr + Plated Grids, No AR Coating).